

Supplementary Material

Mono- and ditopic models of binding of a photochromic chromene annelated with an 18-crown-6 ether with protonated amino acids

Sergey Paramonov, Yury Fedorov, Vladimir Lokshin, Elena Tulyakova, Gaston Vermeersch, Stéphanie Delbaere and Olga Fedorova

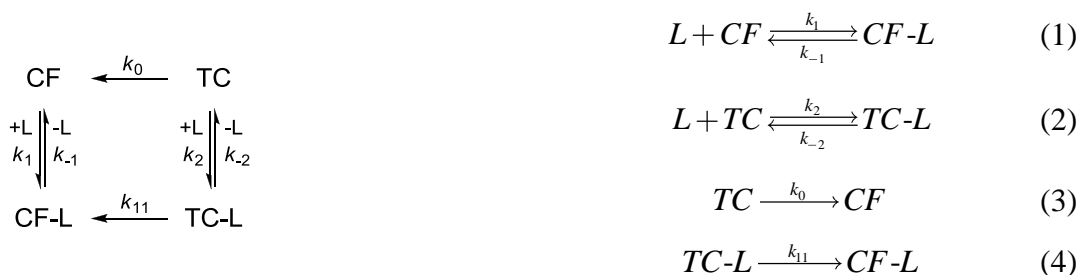
Contents:

| | |
|---|----|
| Kinetic scheme of the bleaching in presence of the ligands | 2 |
| Spectrophotometric titration of 1 by NH ₄ ClO ₄ and C8 (Fig. S1) | 5 |
| NMR data of chromene 1 , amino acid C8 and complex 1b •C8: | |
| Tables S1-S3..... | 6 |
| Figures S2-S9 | 7 |
| NMR monitoring of the thermal relaxation of chromene 1 at 0°C (Figs. S10, S11)..... | 11 |
| UV-Vis studies on the bleaching kinetics of chromene 1 | |
| in the presence of different ligands (Figs. S12-S15)..... | 12 |
| The thermal TC to TT transformation of 1 in the presence of C8 (Fig. S16)..... | 14 |

Kinetic scheme of the bleaching in presence of the ligands

Elaborating the kinetic scheme of the bleaching process, we were following the concepts presented in «Binding Constants: The Measurement of Molecular Complex Stability» (Wiley-Interscience, New York, 1987) and «Chemical Kinetics: The Study of Reaction Rates in Solution» (VCH Publishers, New York, 1990) both by K.A.Connors.

Let us assume that the OFs form only one type of complexes, namely the 1:1 species. In this case, seven components would virtually be present in the solution after the irradiation is cut. They are (1) the CF, (2) the TC and (3) TT forms, (4) the free ligand (*L*), (5) the CF, (6) TC, and (7) TT complexes. As it was mentioned earlier, we used a short term irradiation that allowed us to obtain the TC form in much greater excess over the TT form (it was also evidenced by the monoexponential pattern of the bleaching curve). So, in our further considerations we will omit the TT form and its complexes. Thus, instead of seven species we would virtually have five of them. Below is the principal scheme that describes the equilibria in the solution during bleaching:

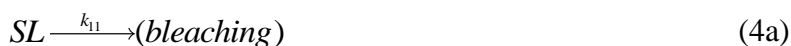


Equations 1 and 2 describe the complex formation between the chromene (CF and TC) and the ligand. Equations 3 and 4 correspond to the thermal bleaching.

We assume that the rate, with which the complex equilibrium is reached, is much faster than the bleaching rate. (This assumption is partly supported by our observations: the addition of the ligand led to the immediate change of the absorption spectrum whereas the bleaching process could be observed during notable period of time, e.g. see half-life time values in Table 3.)

As we measure the bleaching rate, i.e. the rate of the disappearance of the TC and TC-L, the products of these reactions do not matter (however, we bear in mind that the reactions proceed via equations 3 and 4). Moreover, we cannot accurately control the accumulation of the CF and CF-L as they absorb in the UV region as well as the TC and TC-L (the same considerations are valid for the measurement of the free ligand concentration). On the contrary, only the latter two species have very distinct absorption bands at about 400 and 500 nm. So, to develop a kinetic scheme we use equations 3 and 4; equation 2 is also important as it sets the relation between the free TC and the TC complex. To simplify the notation, let us denote the TC form as *S*, the substrate. Consequently, the 1:1 complex will be written as *SL* and the equation 2-3 will be rewritten as follows:





The differential equation determining the rates of the two bleaching reactions are

$$-\frac{d[S]}{dt} = k_0[S] \quad (5)$$

$$-\frac{d[SL]}{dt} = k_{11}[SL] \quad (6)$$

where square brackets denote the equilibrium concentration of the components.

Taking into account that these two processes occur simultaneously, one should virtually observe a biexponential decay. In our case, the decay was essentially monoexponential (not to be confused with the TT formation) characterized by the observed rate constant k_{obs} . Thus, we suppose that the overall concentration of the substrate C_S (free and complexed) is changing via a pseudo-first-order law

$$-\frac{dC_S}{dt} = k_{obs}C_S \quad (7)$$

Combining equations 5-7 gives

$$k_{obs}C_S = k_0[S] + k_{11}[SL] \quad (8)$$

The equation for the stability constant and the mass balance equation set the relation between the equilibrium concentrations of all the species:

$$K_{11} = \frac{[SL]}{[S][L]} \Rightarrow [SL] = K_{11}[S][L] \quad (9)$$

$$C_S = [S] + [SL] = [S] + K_{11}[S][L] \quad (10)$$

Using equations 9 and 10 in 8 gives the general formula for k_{obs}

$$k_{obs} = \frac{k_0[S] + k_{11}[SL]}{C_S} = \frac{k_0[S] + k_{11}K_{11}[S][L]}{[S] + K_{11}[S][L]} = \frac{k_0 + k_{11}K_{11}[L]}{1 + K_{11}[L]} \quad (11)$$

In the course of titration, a large excess of the ligand was used. Therefore, it may be assumed that $[L] = C_L$:

$$k_{obs} = \frac{k_0 + k_{11}K_{11}C_L}{1 + K_{11}C_L} \quad (\text{eq. 1})$$

where C_L is the total concentration of the ligand.

Suppose the 1:1 complex bind another ligand molecule:



where SL_2 denotes the 1:2 complex.

In this case, taking into consideration the same assumptions, a new bleaching process will be involved and the kinetic scheme will be extended by the following equations:

$$K_{12} = \frac{[SL_2]}{[SL][L]} \Rightarrow [SL_2] = K_{12}[SL][L] \quad (13)$$



$$C_S = [S] + [SL] + [SL_2] \quad (10a)$$

$$k_{obs} C_S = k_0[S] + k_{11}[SL] + k_{12}[SL_2] \quad (8a)$$

$$k_{obs} = \frac{k_0 + k_{11}K_{11}[L] + k_{12}K_{11}K_{12}[L]^2}{1 + K_{11}[L] + K_{11}K_{12}[L]^2} \quad (11a)$$

$$k_{obs} = \frac{k_0 + k_{11}K_{11}C_L + k_{12}K_{11}K_{12}C_L^2}{1 + K_{11}C_L + K_{11}K_{12}C_L^2} \quad (\text{eq. 2})$$

The rate constants were determined from the UV-Vis experiments. With each new addition of the ligand, the decay of the absorbance at 385 nm was recorded (e.g. Figs. 8a, 9a-c, S12a,b) and then fitted to a generic decay formula

$$y = y_1 e^{-ax} + y_2 e^{-bx} \quad (15)$$

where the two components correspond to the bleaching of the TC and TT, respectively. (This biexponential decay should not be attributed to the bleaching of the free and complexed OF. There are two main factors that support this assumption. First, the difference in the rate constant values which if plotted do not follow any rational trend. Second, the observation of the TT formation in NMR.)

On each titration step, the exponential coefficients a and b (if applicable) were determined. Afterwards the values of a and b (if applicable) were plotted against C_L and the obtained data set was fitted to either eq. 1 or eq. 2 (see Figs. S12-S15).

It should be also noted that we have not determined the molar extinctions for the free and complexed OFs.

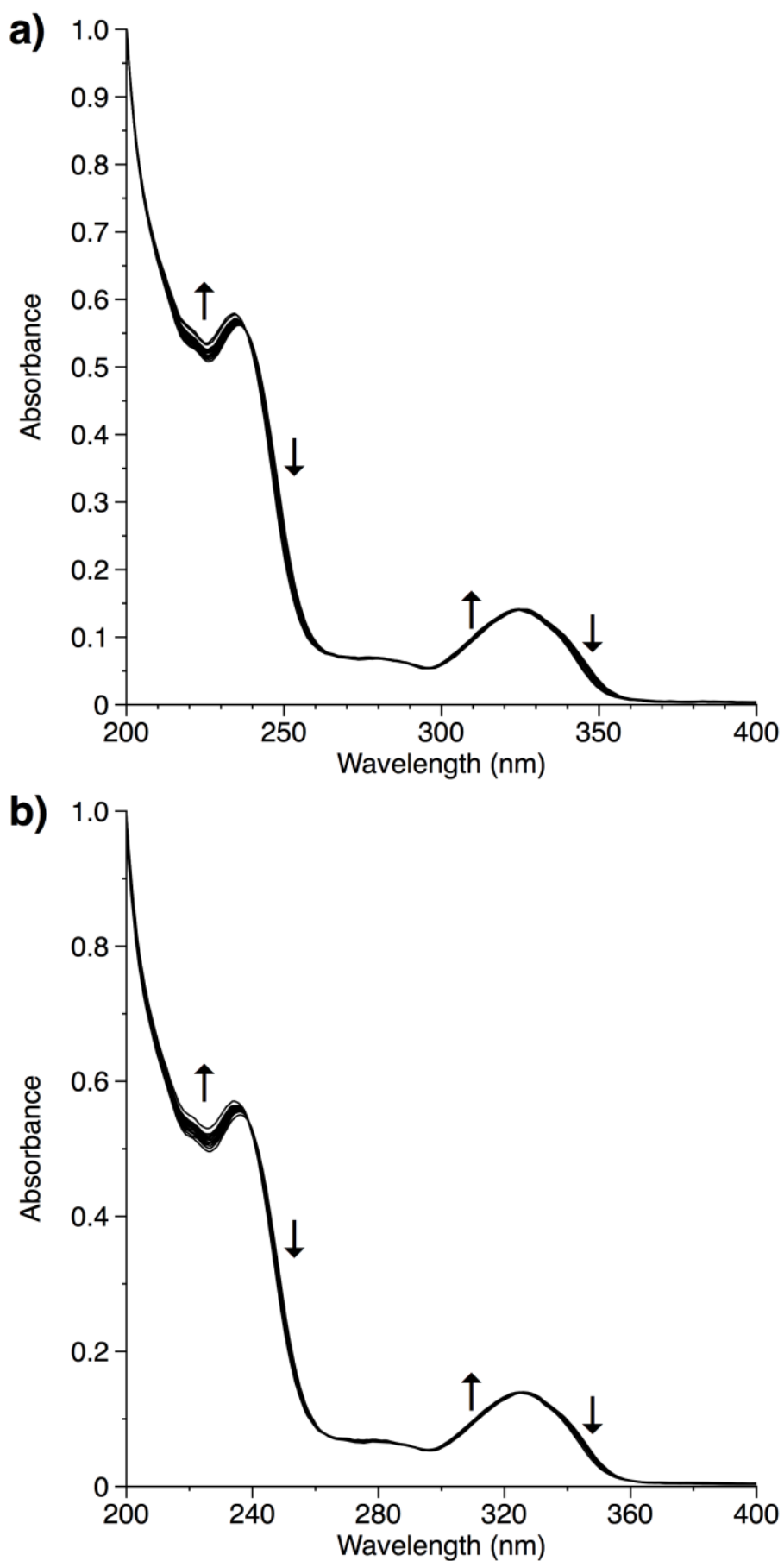


Figure S1. Spectrophotometric titration of chromene **1** by ammonium perchlorate (a) and protonated ω -aminocaprylic acid (b) in acetonitrile. $C_1 = 2 \times 10^{-5}$ M, $C_L/C_1 = 0 \rightarrow 8$ (C_L is NH_4ClO_4 or C8 concentration).

Table S1. The chemical shifts of chromene **1b**, amino acid C8 and complex **1b•C8** at 295 K in ^1H NMR spectra in CD_3CN at 500 MHz spectrometer.

| Compound | Chemical shift / ppm | | | | | | | | | | | | | | |
|--------------|----------------------|------|------|------|------|---------------|---------------|------|------|------------------|-------|-------|-----------------|-------|-------|
| | H-2' | H-3' | H-4' | H-3 | H-4 | H-5, 22 | H-7,20 | H-8 | H-19 | H-11, 13, 14, 16 | H-2'' | H-3'' | H-4'', 5'', 6'' | H-7'' | H-8'' |
| 1b | 7.44 | 7.33 | 7.26 | 6.23 | 6.59 | 6.62 | 4.11 | 3.72 | 3.68 | 3.61–3.78 | – | – | – | – | – |
| C8 | | | | – | – | – | – | – | – | – | 2.27 | 1.59 | 1.33 | 1.59 | 2.92 |
| 1b•C8 | 7.44 | 7.32 | 7.27 | 6.27 | 6.61 | 6.71, 6.74 | 4.18, 4.09 | 3.82 | 3.78 | 3.61–3.78 | 1.97 | 1.47 | 1.13 | 1.37 | 2.75 |

Table S2. The coupling constants of several signals of chromene **1b**, amino acid C8 and complex **1b•C8** at 295 K in ^1H NMR spectra in CD_3CN at 500 MHz spectrometer.

| Compound | Coupling constant / Hz | | | | |
|--------------|------------------------|-------|---------|---------|-----|
| | 2'-3' | 3'-4' | 2''-3'' | 7''-8'' | 3-4 |
| 1b | 7.4 | 7.4 | – | – | 9.6 |
| C8 | – | – | 7.5 | 7.7 | – |
| 1b•C8 | 7.7 | 7.5 | 7.6 | 6.7 | 9.7 |

Table S3. The chemical shifts of amino acid C8 and complex **1b•C8** at 295 K in ^{13}C NMR spectra in CD_3CN at 500 MHz spectrometer.

| Compound | Chemical shift / ppm | | | | | | | | | | | | |
|--------------|----------------------|-------|-------|-------|-------|--------|--------|------------------|-------|-------|--------------------|-------|-------|
| | C-2', 3', 4' | COOH | C-3 | C-4 | C-5 | C-7,20 | C-8,19 | C-11, 13, 14, 16 | C-2'' | C-3'' | C-4'', 5'', 6'' | C-7'' | C-8'' |
| C8 | – | 173.4 | – | – | – | – | – | – | 33.1 | 26.8 | 25.4, 28.5 | 24.3 | 40.1 |
| 1b•C8 | 127.3, 127.5 | 174.2 | 127.1 | 122.7 | 109.8 | 67.5 | 68.7 | 69.3 | 33.2 | 26.9 | 26.5 | 24.4 | 39.5 |

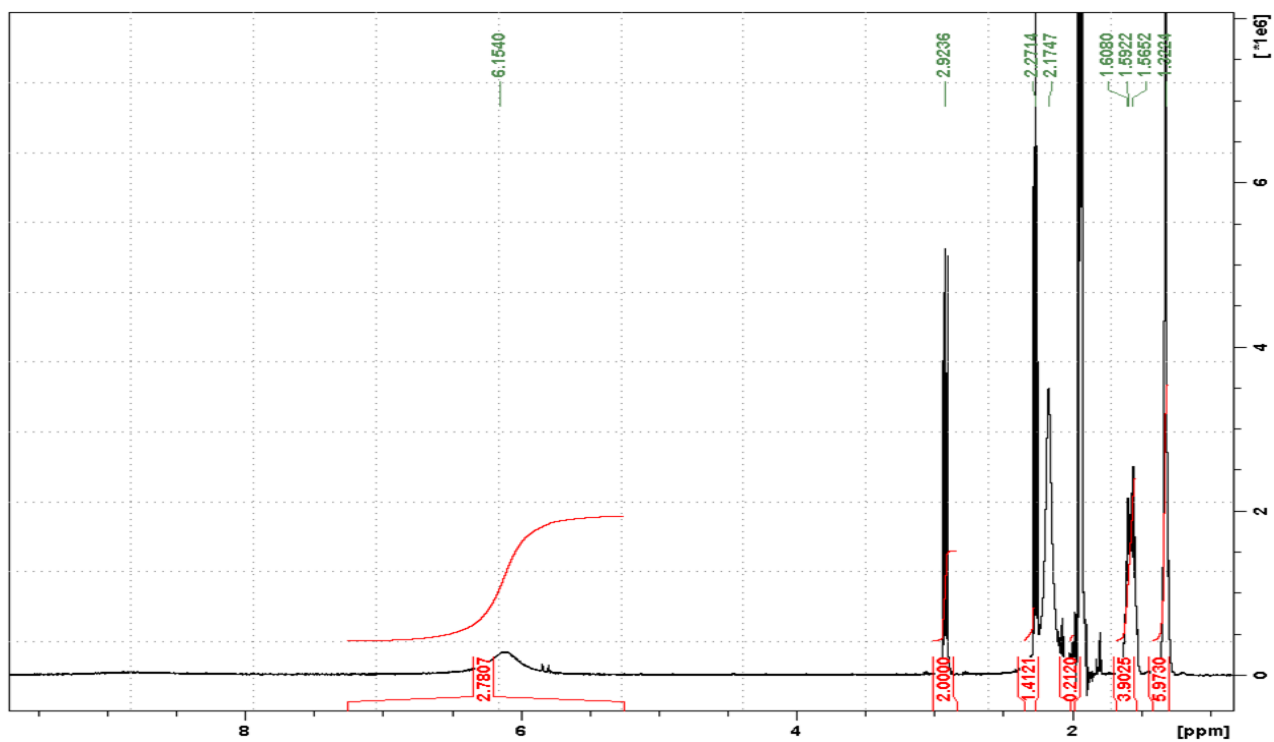


Figure S2. ^1H NMR spectrum of **C8** in CD_3CN at 295 K.

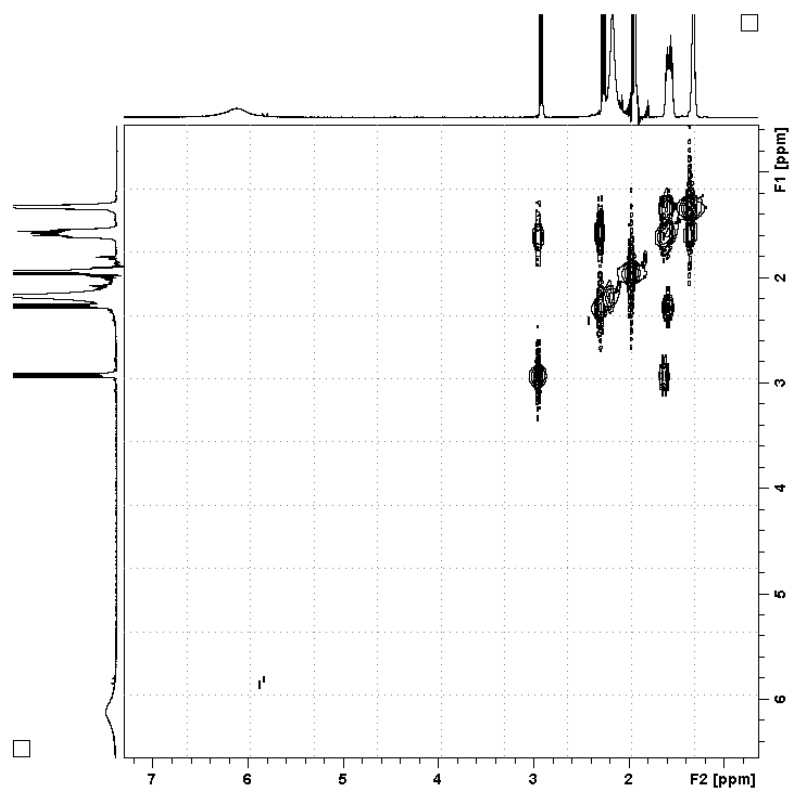


Figure S3. ^1H - ^1H COSY spectrum of **C8** in CD_3CN at 295 K.

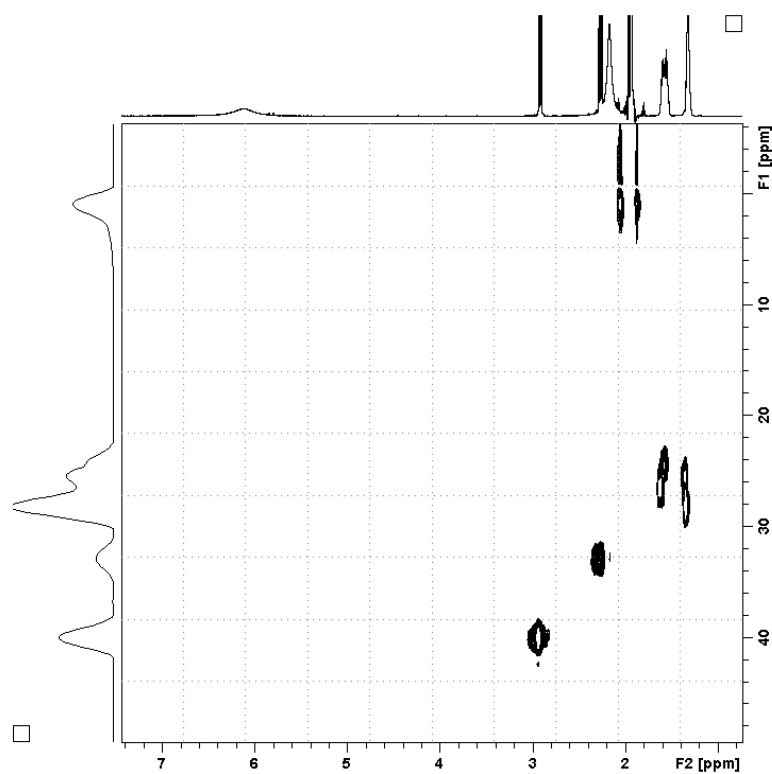


Figure S4. ^1H - ^{13}C HSQC spectrum of C8 in CD_3CN at 295 K.

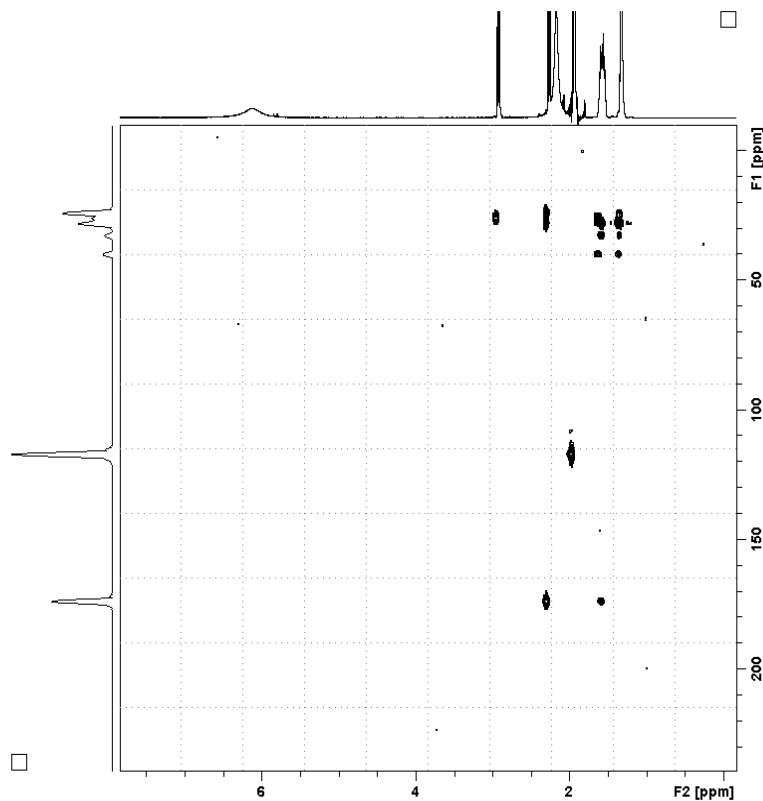


Figure S5. ^1H - ^{13}C HMBC spectrum of C8 in CD_3CN at 295 K.

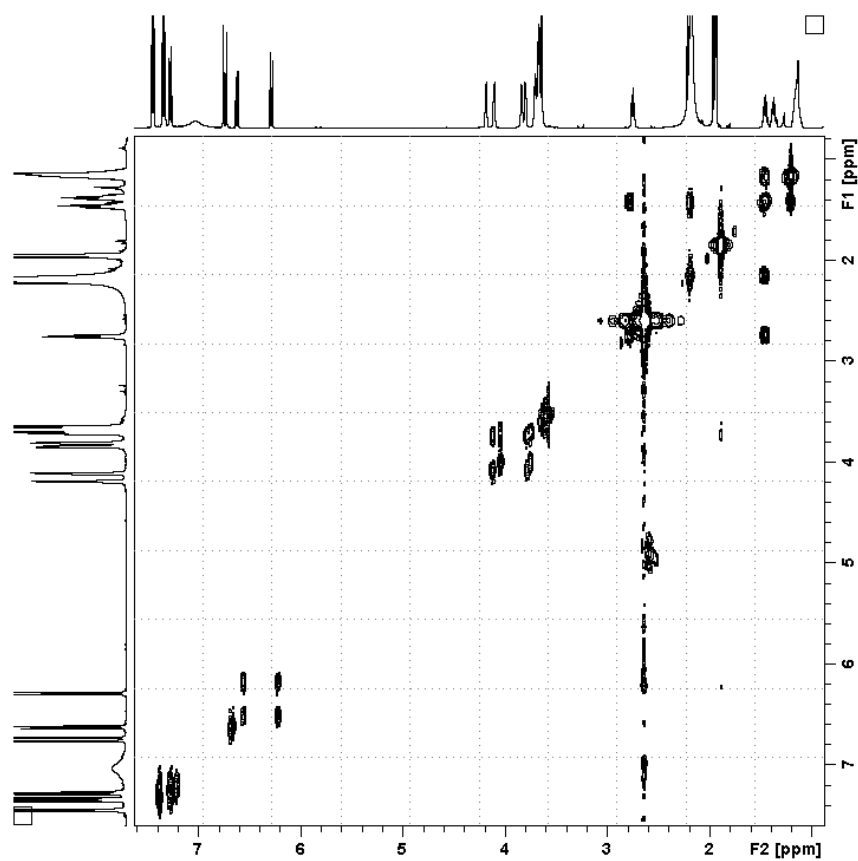


Figure S6. ^1H - ^1H COSY spectrum of the complex **1b•C8** in CD_3CN at 295 K.

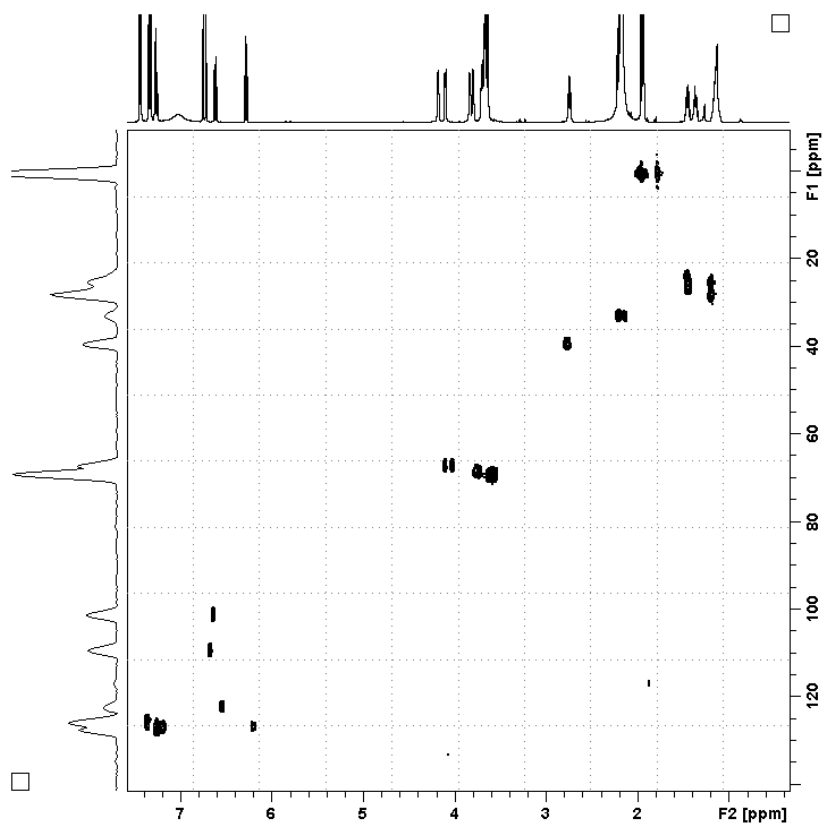


Figure S7. ^1H - ^{13}C HSQC spectrum of the complex **1b•C8** in CD_3CN at 295 K.

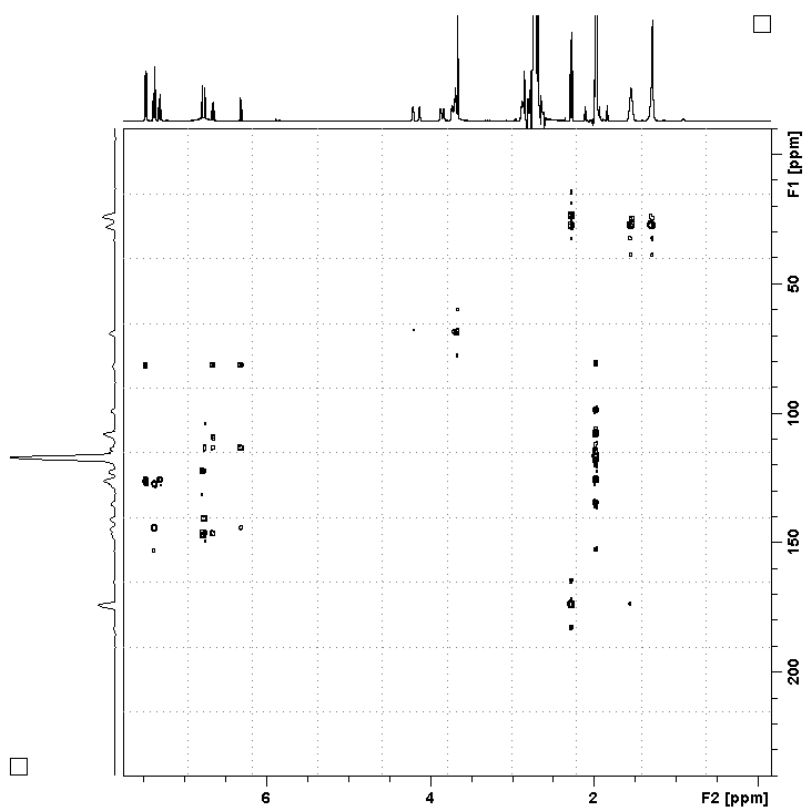


Figure S8. ^1H - ^{13}C HMBC spectrum of the complex **1b**•**C8** with in CD_3CN at 295 K.

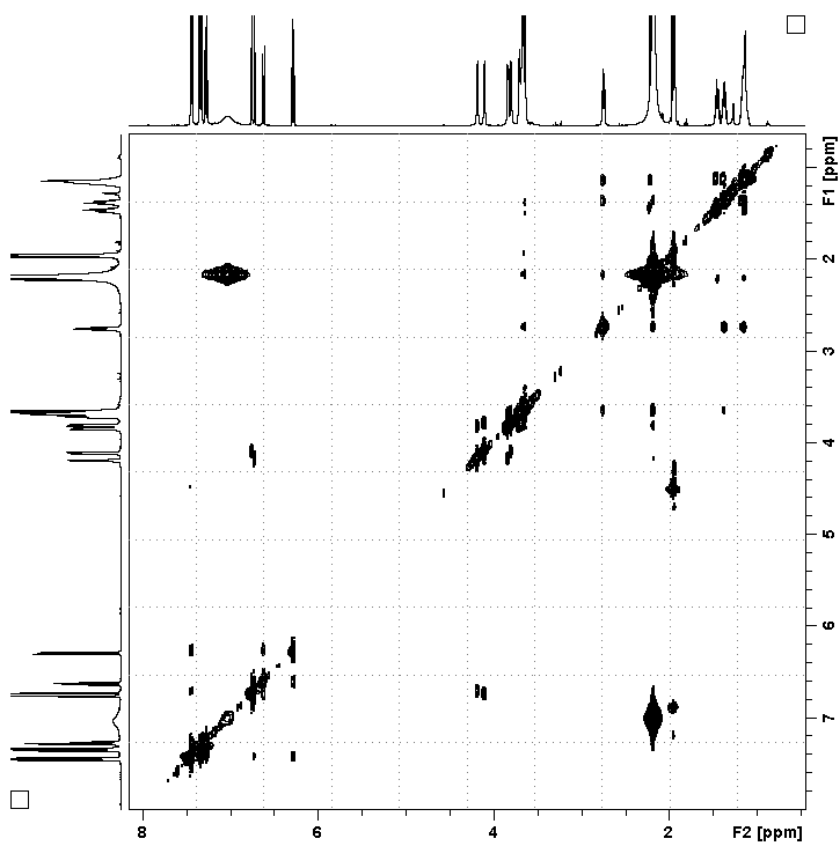


Figure S9. ^1H - ^1H NOESY spectrum of the complex **1b**•**C8** in CD_3CN at 295 K.

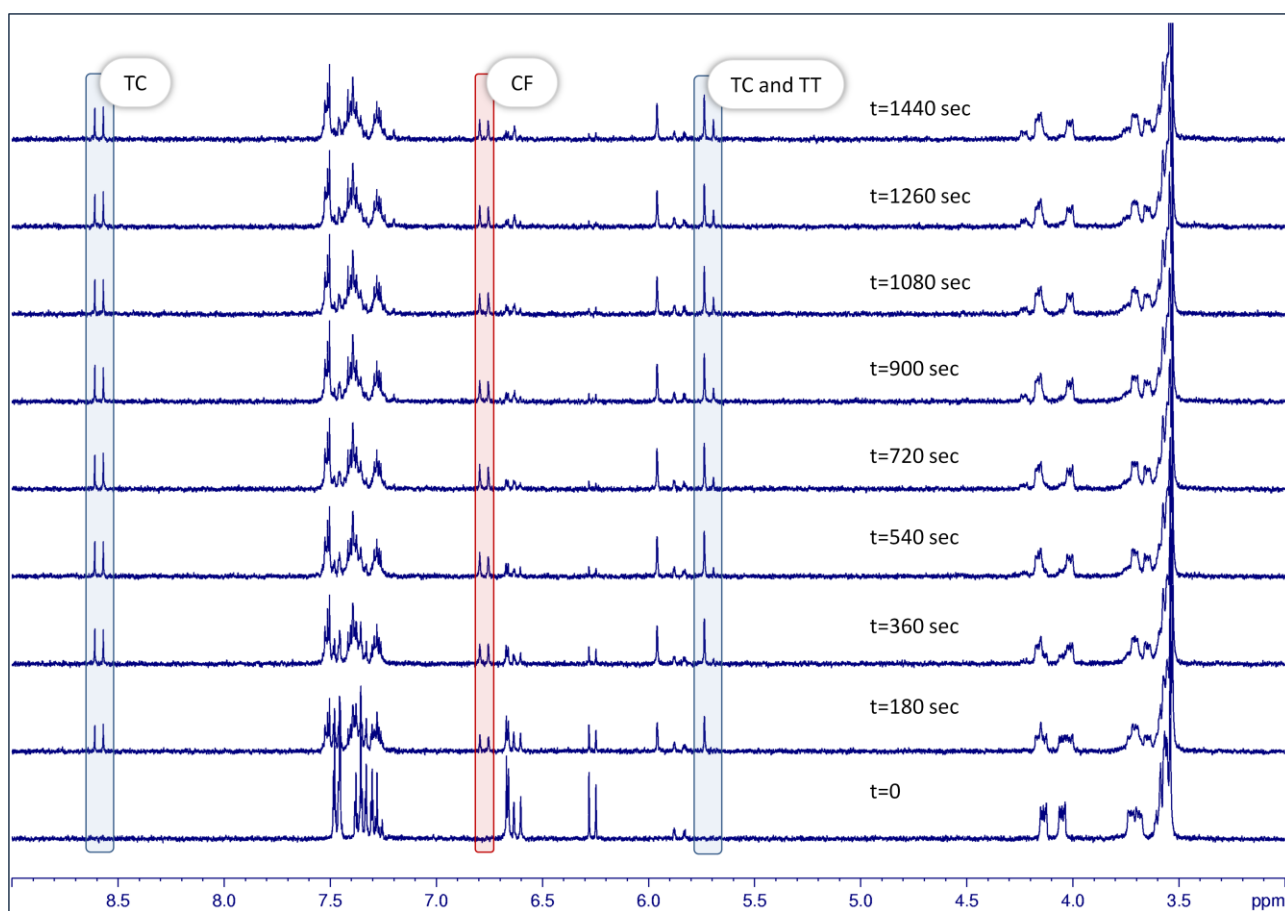


Figure S10. ^1H NMR monitoring of the phototransformation (coloration) of the solution of **1** ($\lambda = 313$ nm, Hg-Xe lamp, 1000W, CD_3CN , 0°C).

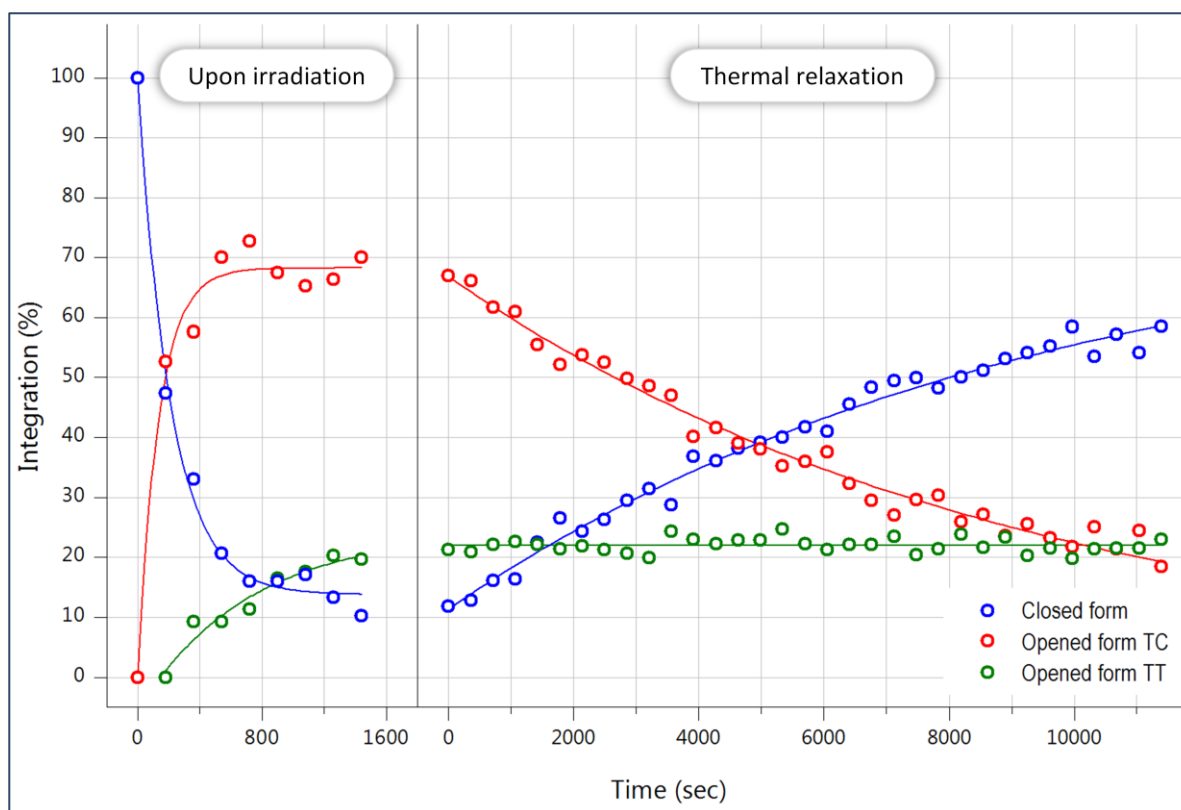


Figure S11. Thermal relaxation of the solution of **1** after irradiation during 24 min at 0°C (see Fig. S9). Bleaching rate constant $k = 1.1 \times 10^{-4} \text{ s}^{-1}$.

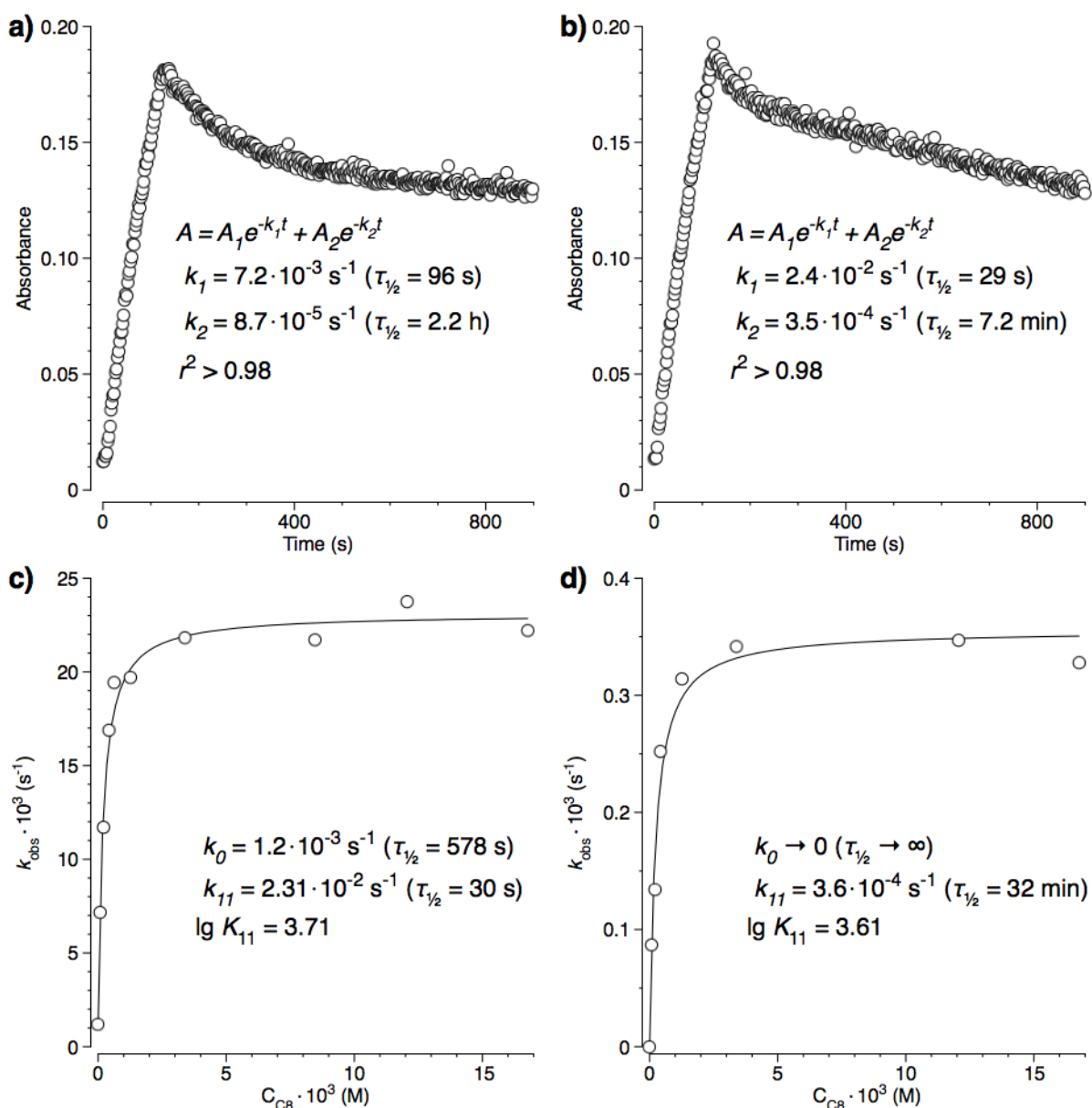


Figure S12. The influence of C8 acid on the bleaching kinetics of chromene 1 solution after irradiation (acetonitrile, $C_1 = 4.2 \times 10^{-3} \text{ M}$, 20°C): a) $\lambda = 385 \text{ nm}$, $C_{C8}/C_1 = 2$; b) $\lambda = 385 \text{ nm}$, $C_{C8}/C_1 \approx 300$; c) and d) dependencies of the observed rate constant of the TC and TT forms, respectively, on the amino acid concentration.

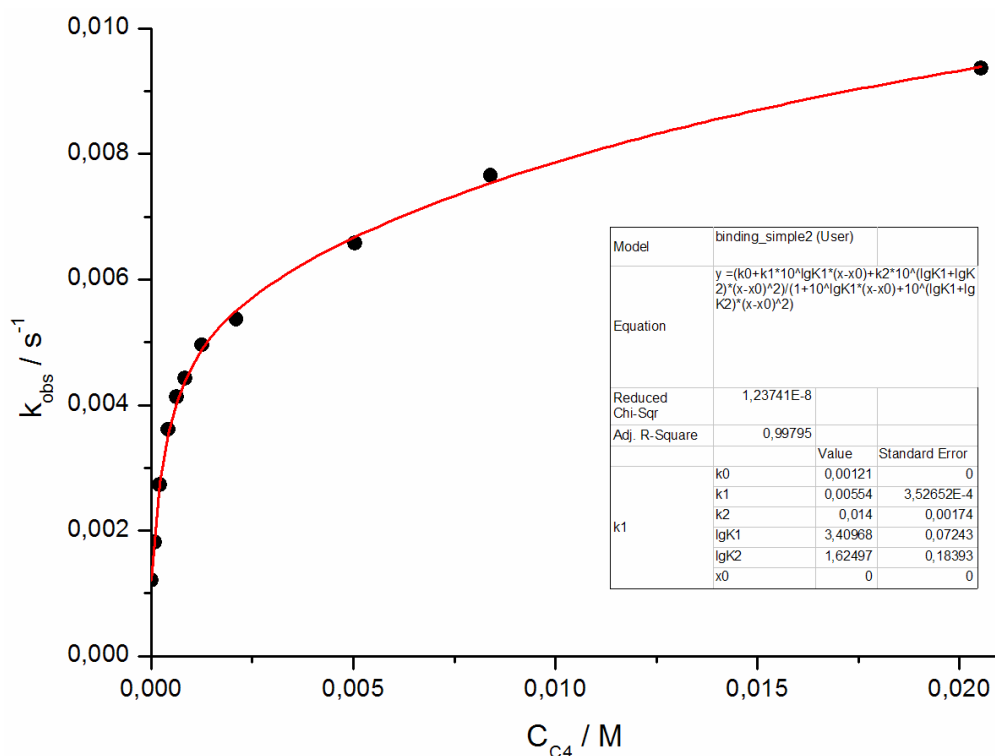


Figure S13. The effect of γ -aminobutyric acid (C4) on bleaching kinetics of **1** solution after irradiation (acetonitrile, $C_1 = 4.2 \cdot 10^{-5}$ M, 20°C): dependence of observed relaxation rate constant of the TC form on amino acid concentration.

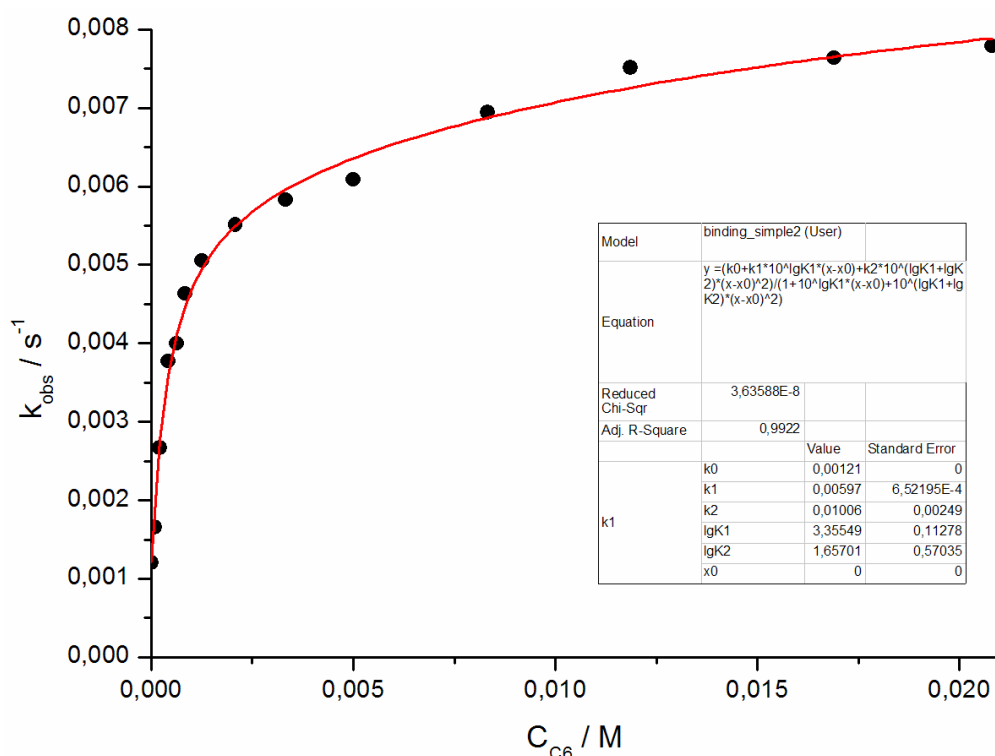


Figure S14. The effect of ϵ -aminocaproic acid (C6) on bleaching kinetics of **1** solution after irradiation (acetonitrile, $C_1 = 4.2 \cdot 10^{-5}$ M, 20°C): dependence of observed relaxation rate constant of the TC form on amino acid concentration.

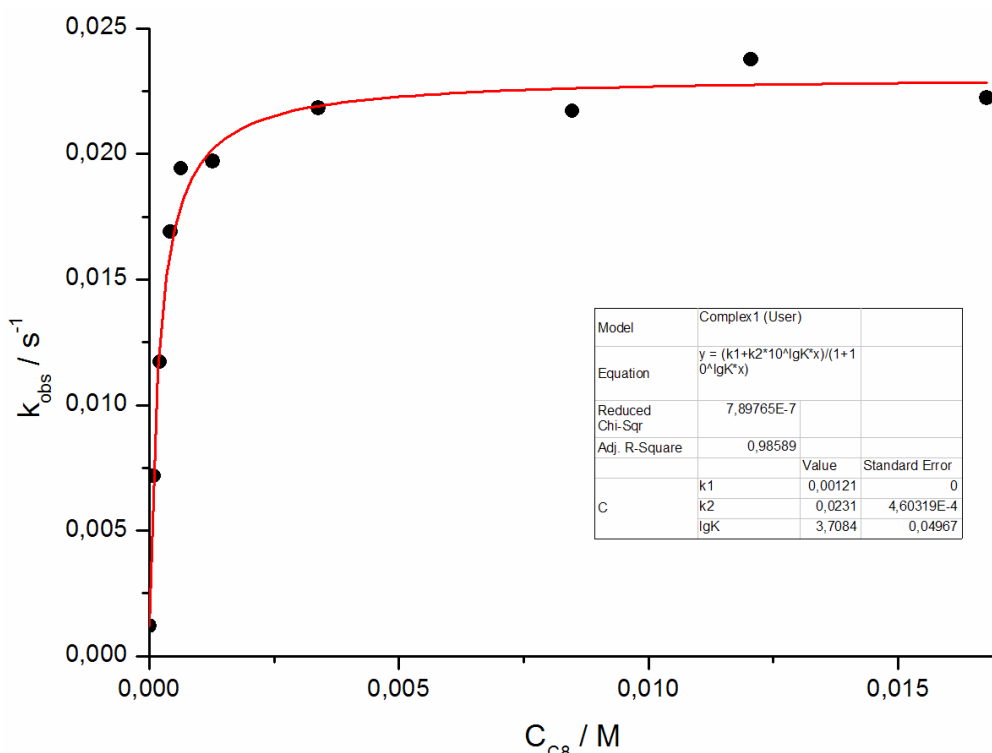


Figure S15. The effect of ω -aminocaproic acid (C8) on bleaching kinetics of **1** solution after irradiation (acetonitrile, $C_1 = 4.2 \cdot 10^{-5}$ M, 20°C): dependence of observed relaxation rate constant of the TC form on amino acid concentration.

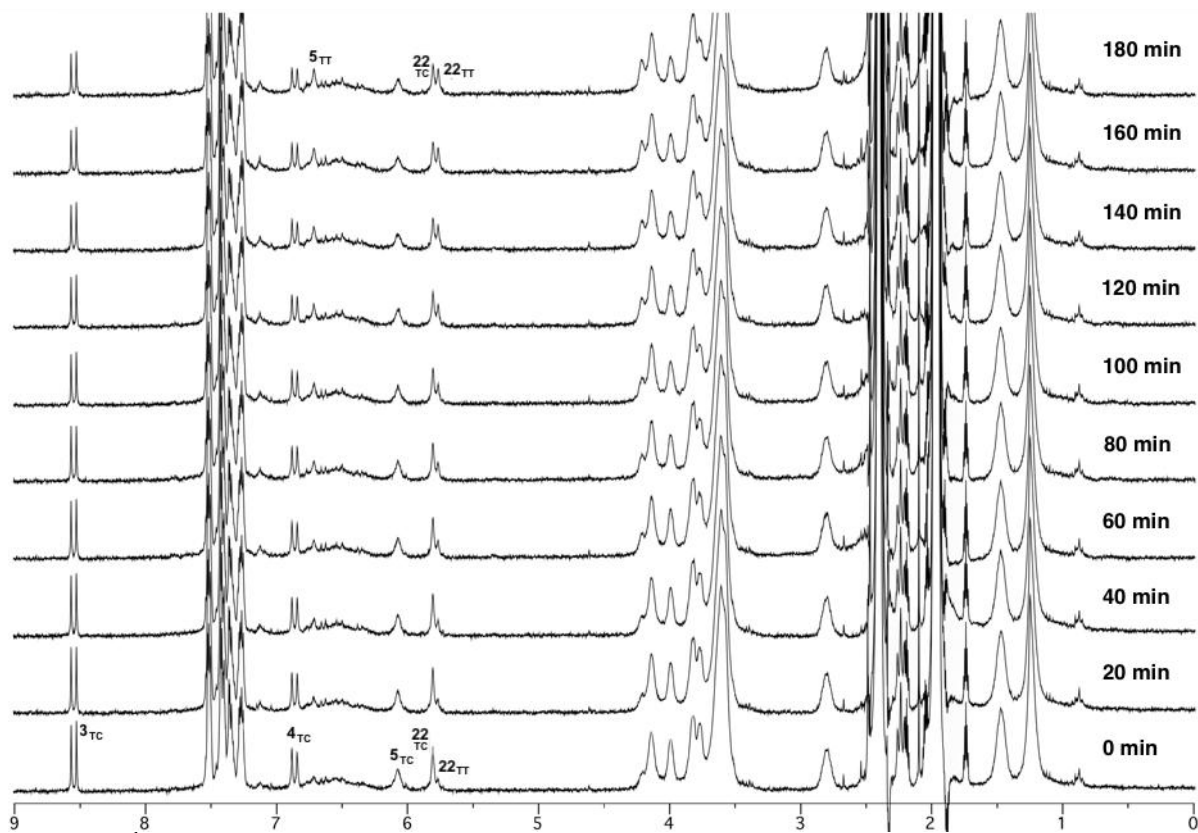


Figure S16. ^1H NMR monitoring of the thermal relaxation of **1** + C8 solution (equimolar concentrations) after 10 min irradiation (CD_3CN , -45°C).